# Continuous gas lift studies for circulation of heavy liquid metal using CFD

**Santosh Kumar Mishra[1*], H. Chandra[2] and Arun Arora[1]**
[1]Mechanical Engg. Dept., B.I.T. Durg, CG, India
[2]Department of Mechanical Engg., V.E.C. Lakhanpur, Sarguja University, Ambikapur, C.G., India
san810@gmail.com

## Abstract

*The spallation target is a key component of the Accelerator Driven System (ADS) and is the source of neutrons resulting from the interaction between the accelerated proton beam (~ GeV) and a heavy density liquid metal target like lead-bismuth eutectic (LBE). The aim of this study is to estimation of various parameters which affects the circulation of heavy density liquid metal like LBE via bouncy driven flow system. Various possible configurations presented to establish the flow of LBE in spallation target module. The analysis has done for circulation of liquid in target using gas lift mechanism. The time dependent studies have been carried out consisting of, riser, two-phase flow region of the riser (for gas driven target), down-comer, rise of free surface etc has been done. All the simulations have been carried out using commercial CFD codes.*

**Keywords:** Continuous flow gas lift, Gas injection rate, CFD, Gas lift optimization, Slip.

## Introduction

Advanced nuclear power reactors called Accelerator Driven Sub-critical Systems (ADS)[1,2,3,4] are being developed mainly for thorium utilization and transmutation of long-lived wastes. At present there are very few accelerators, which can give few mA and high-energy proton beam. However, accelerators with low energy (tens of MeV)[5] and hundreds of micro-ampere current are commercially available. In view of this, it has been proposed to use these commercially available accelerators to simulate window heating to study various thermo-mechanical issues of window. The target geometry considered in the present simulation is shown in Figure-1. The proton beam comes from the top through the inner pipe and impinges on the window. Lead Bismuth Eutectic (LBE) has been chosen as the target material[6]. The same LBE also acts as the coolant[12]. LBE enters from below and leaves from the top through the annular space between the concentric pipes. The LBE circulation is maintained by gas-injection. 15 kW of heat deposition (650 MeV, 500μA proton beam with flat profile) and LBE flow rates of 30 to 40 kg/s have been considered. The spallation target acts as the external neutron source and is the key component of this system. The design of the window, a physical barrier separating the liquid metal from the proton beam, is crucial as it is subjected to thermal stresses (apart from the mechanical stresses due to pressure and drag of the liquid metal) due to high heat fluxes and heat deposition within it. The window needs to be designed for separating high vacuum conditions of proton beam channel and the molten target environment and hence, it must be thin yet with adequate mechanical strength. It is also essential to study the thermal-hydraulics of the spallation region in the target where a large amount of heat is generated due to the nuclear interaction with the liquid metal target. However, for the proton beam considered here there is no spallation nuclear reaction and heat deposition is due to Columbic interaction only. So the total heat is deposited in the beam window itself. Circulating LBE has to extract around 15 kW[1] of heat deposited by the beam in the window.

## Materials and methods

Prior to simulation, the spallation target was modeled by GAMBIT 2.3.16 with a few assumptions and boundary condition that will be described detailed in next section. Then, the simulation process was carried out with FLUENT 6.3.26.

**Modelling the spallation target:** Spallation target for gas lifts was modeled by, GAMBIT 2.3.16 with all assumptions and boundary condition being made as described in the next section. The study consists of a spallation target which is filled with liquid metal LBE at certain level and gas (non reactive gas such as helium or Nitrogen) enters at the specific injection port at certain height in the domain. The liquid metal was selected as primary phase(continuous fluid) in the system while the injected gas was being well specify by determine the specific rate needed to produce required velocity of liquid metal treated as Secondary fluid (dispersed fluid). Table-1 shows the properties of the liquid metal (Lead Bismuth Eutectic) and gas while various parameter that affects the flow of mixture showed in Table-2.

It is not possible to generate structured grid for the considered target geometry, so block structured grid with 10000 quadrilateral cells has been generated. The mesh interval size used is 0.5 mm. The grid at the inlet, outlet is meshed with interval size of 0.25 mm so at least 20 cells are available for calculation in the gas outlet regions. The computation is done by parallel processing (2 dual processor nodes) and it took around 90 hrs to complete one simulation.
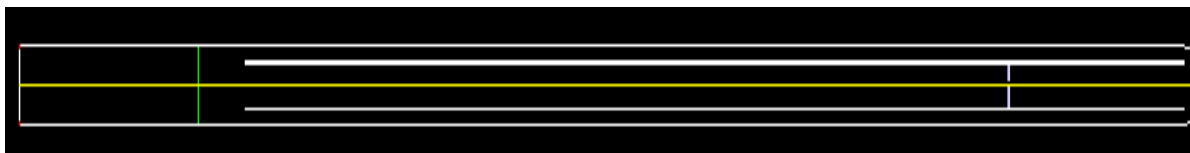
**Figure-1:** Target geometry for simulation.

**Table-1:** Properties of the component.

| Component | Density (kg m$^{-3}$) | Viscosity (Pa s) |
|---|---|---|
| Liquid Metal (LBE) 45% lead and 55% bismuth | 1640 | 1.654x10$^{-6}$ |
| Nitrogen | 1.1576397225 | 17.6885696x10$^{-6}$ |

**Table-2:** Following parameter possibly affects the flow of (liquid and gas) mixture.

| Parameter | Value |
|---|---|
| Mass flow rate of Gas (gm s$^{-1}$) | 0.5, 1.0, 1.5, 2.0 |
| Depth of free liquid surface from the Gas outlet (mm) | 750, 937.5 |
| Gas Bubble Diameter (mm) | 2.5, 5, 10, 15 |
| Width of Down comer Zone (mm) | 22, 33, 44 |
| Gas outlet opening (mm) | 5, 20 |
| Spallation target with and without heat exchanger (length of heat exchanger in mm) | 4200 |
| Number of gas Mixer | 5, 10 |
| Gap Between Inner pipe and spherical end | 10, 70 |

**Model assumptions and limitations**[7,8]**:** In order to proceed with the simulation, several assumptions need to be applied in this study based on the software criteria and limitations as stated below: i. Negligible of formation gas in volume and pressure. ii. Injection gas pressure was higher than the Bottom Head as it was low where gas injection was needed. iii. Gas entered the tubing were assumed uniformly distributed at the inlet cross section while the mixture of liquid metal and gas was assumed to be homogenous mixture before reaching the model boundary maximum length at 3 meters. iv. Radius of gas inlet was set at 1/3 of radius of spallation target size since varying the diameter of target without careful calculations will lead to divergence in iteration. v. The spallation target was packed off in this study otherwise simulations require set up of a porous zone or liquid zone outside the setup bottom boundary. vi. Single string of gas injection was used to avoid the complicated multi phase flow

and existence of secondary flow. vii. The atmospheric pressure was 0.1 MPa while the gravitational acceleration was 9.81 ms$^{-1}$.

**Simulation process**[9]**:** 3D segregated 1st order implicit solver approach, was used for solving the set of governing equations for multi-phase calculations, Ansys Fluent 16.2 is used for the analysis. Using the segregated solver, the flow of multi phase flow of liquid and gas should be accept as in unsteady state. The standard k-ε mixture multi phase model was used to treat turbulence phenomena in both phases. Energy Equation is turned off. Flow regime corresponding to analysis is mostly bubbly flow (i.e. void fraction is less than 0.25). For this type of flow regime best suitable model is Eulerian multiphase model. In this model phases are taken explicitly and separate equations are written for each phase and the interaction between the phases is also considered. Different properties and velocities for each phase has been considered by this model. The simulation was focus more on the velocity magnitude of the flowing fluids. Both contour and vector of the fluid will be process from the result and the residual plot is turn on during the simulation. The modelling and simulation involves following steps to ensure the result convergence thus valid to be used[10,11]: i. Multi blocked structure grid generation if possible. ii. Transform governing equation into algebraic equations for each element. iii. Discretization schemes selection. iv. Discretized equation at every grid location. v. Pressure and continuity equation formulation. vi. Selection of suitable iteration scheme for obtaining a final solution.

For each Phase continuity, momentum, and energy equation are written. Six equations are than solved simultaneously, together with the rate equations, Phases interact with each other and with the walls of the duct by taking care with these equations. In the simplest analysis only one parameter (usually velocity) is allowed to differ for the two phases while conservation equations are only written for the combined flow.

**Governing Equations**[12,10]**:** The flow is assumed to be turbulent and incompressible. The buoyancy effect is neglected. The governing equations are written in Cartesian x-y co-ordinates.

**Volume fraction equation:** Volume fractions represent the space occupied by each phase, and the laws of conservation of mass and momentum are satisfied by each phase individually. The derivation of the conservation equations can be done by ensemble averaging the local instantaneous balance for each of the phases. The volume of phase $q$, $V_q$ is defined by

$$V_q = \int_V \alpha_q \, dV \qquad (1)$$

$$\sum_{q=1}^{n} \alpha_q = 1 \qquad (2)$$

The effective density of phase $q$ is $\hat{\rho}q = \alpha_q \rho_q$ Where, $\rho_q$ is the physical density of phase $q^{th}$. In a two-phase system, the phases are represented by the subscripts 1 is liquid phase (continuous fluid) and 2 is gas phase (dispersed fluid).

**Mass Conservation:** The continuity equations for the phases can be written as,

$$\frac{\partial}{\partial t}(\alpha_q \rho_q) + \nabla.(\alpha_q \rho_q \vec{v}_q) = \sum_{q=1}^{n}(\dot{m}_{pq} - \dot{m}_{qp}) + S_q \qquad (3)$$

**Conservation of Momentum**: The momentum balance for phase q yields

$$\frac{\partial}{\partial t}(\alpha_q \rho_q \vec{v}_q) + \nabla.(\alpha_q \rho_q \vec{v}_q \vec{v}_q) = -\alpha_q \nabla p + \alpha_q \rho_q \vec{g} \; + \\ \sum(\vec{R}_{pq} + \dot{m}_{pq}\vec{v}_{pq}) + M_{qp} + \nabla.\alpha_q(\tau_q + \tau_q^R) \qquad (4)$$

$\vec{R}_{pq}$ is an interaction force between phases, and p is the pressure shared by all phases. $\vec{v}_{pq}$ is the interphase velocity, defined as follows. If $\dot{m}_{pq} > 0$ (i.e., phase p mass is being transferred to phase q), $\vec{v}_{pq} = \vec{v}_p$; If $\dot{m}_{pq} < 0$ (i.e., phase q mass is being transferred to phase p), $\vec{v}_{pq} = \vec{v}_q$;

Likewise, if $\dot{m}_{qp} > 0$ then it suggests $\vec{v}_{qp} = \vec{v}_q$

To achieve the objective, the simulation was run with deferent mass flow rate of gas for given sets of spallation target geometry listed in Table-3.

**Table-3:** Various configurations of model used in simulation.

| No | Mass flow rate of gas (gm s$^{-1}$) | Depth of free liquid surface from the Gas outlet (mm) | Gas Bubble Diameter (mm) | Width of Down comer Zone (mm) | Gas outlet opening (mm) | Number of gas Mixer | Gap Between Inner pipe and spherical end (mm) | With or without HX |
|---|---|---|---|---|---|---|---|---|
| SET 01 | 0.5 | 750 | 5 | 22 | 5 | 5 | 70 | |
| SET 02 | 1.0 | 750 | 5 | 22 | 5 | 5 | 70 | |
| SET 03 | 1.5 | 750 | 5 | 22 | 5 | 5 | 70 | |
| SET 04 | 2.0 | 750 | 5 | 22 | 5 | 5 | 70 | |
| SET 05 | 0.5 | 750 | 5 | 22 | 20 | 5 | 70 | |
| SET 06 | 0.5 | 750 | 5 | 44 | 20 | 5 | 70 | |
| SET 07 | 1.0 | 750 | 5 | 44 | 20 | 5 | 70 | |
| SET 08 | 1.5 | 750 | 5 | 44 | 20 | 5 | 70 | |
| SET 09 | 2.0 | 750 | 5 | 44 | 20 | 5 | 70 | |
| SET 10 | 0.5 | 937.5 | 5 | 44 | 20 | 10 | 10 | √ |
| SET 11 | 1.0 | 937.5 | 5 | 44 | 20 | 10 | 10 | √ |
| SET 12 | 1.5 | 937.5 | 5 | 44 | 20 | 10 | 10 | √ |
| SET 13 | 2.0 | 937.5 | 5 | 44 | 20 | 10 | 10 | √ |
| SET 14 | 2.2 | 937.5 | 5 | 44 | 20 | 10 | 10 | √ |
| SET 15 | 2.0 | 937.5 | 5 | 44 | 20 | 10 | 70 | √ |
| SET 16 | 0.5 | 937.5 | 5 | 33 | 20 | 10 | 10 | √ |
| SET 17 | 1.0 | 937.5 | 5 | 33 | 20 | 10 | 10 | √ |
| SET 18 | 2.0 | 937.5 | 5 | 33 | 20 | 10 | 10 | √ |
| SET 19 | 2.2 | 937.5 | 5 | 33 | 20 | 10 | 10 | √ |
| SET 20 | 1.0 | 937.5 | 2.5 | 33 | 20 | 10 | 10 | √ |
| SET 21 | 1.0 | 937.5 | 10 | 33 | 20 | 10 | 10 | √ |
| SET 22 | 1.0 | 937.5 | 15 | 33 | 20 | 10 | 10 | √ |

## Results and discussion

The bubble diameter for defining nitrogen phase is taken as 5.0mm. Figure-2 it was seen that nitrogen is trapped in the recirculation zone. However, it was also seen that the amount of gas moving out of the trapped region is also increasing. There was a higher amount of gas entrapped near the wall due to adhesion to the wall. This is in accordance with the theoretically predicted phenomenon. Nitrogen separates at end of inner wall

in riser and flows out of domain through outlet. So nitrogen occupies space above LBE. For minimum flow rate of nitrogen maximum flow rate of LBE was 31 kg/s with carry-under, as $N_2$ flow rate increased LBE flow rates decreased with increasing the free surface height because void fraction increases with gas flow rate so extra gas displaces the liquid, shown in Figure-2, At 2 gm/s of $N_2$, LBE going out from the pressure outlet.
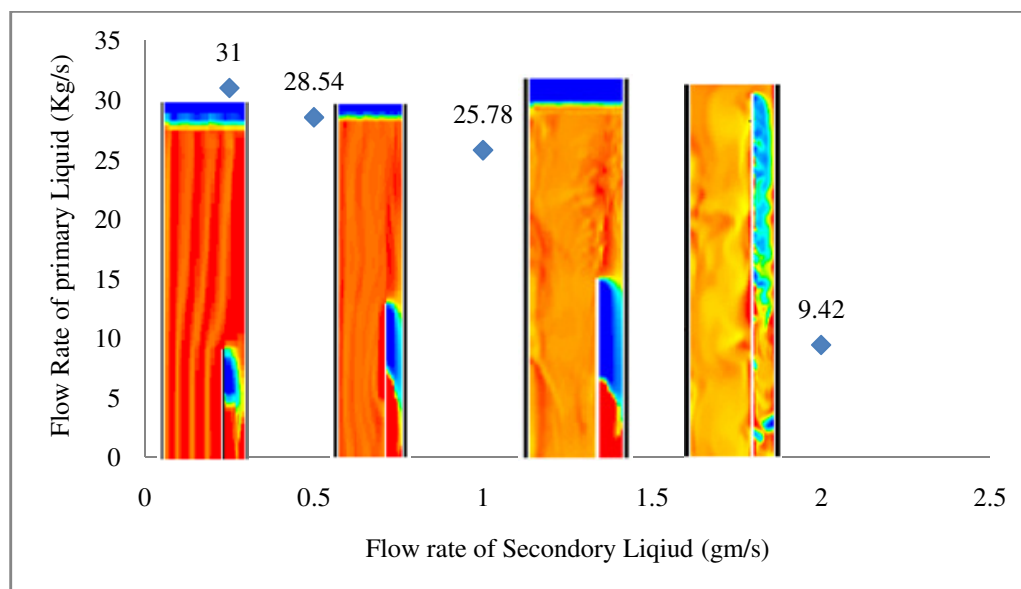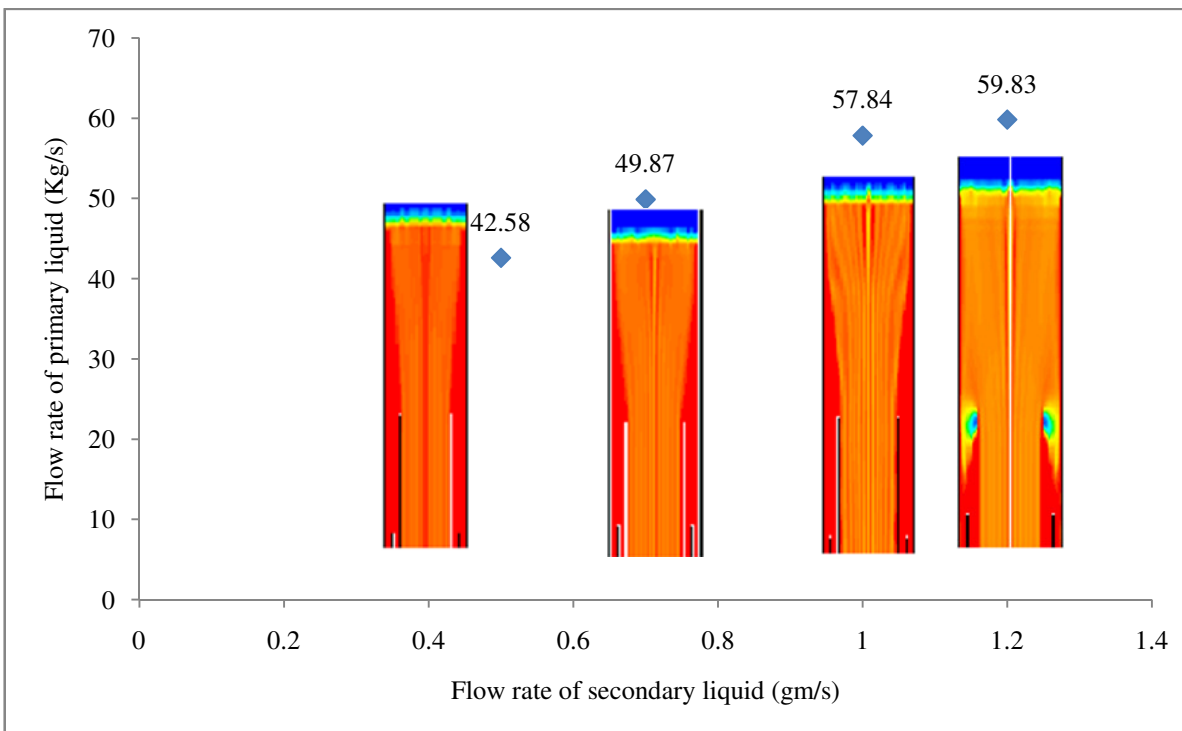


**Figure-2(a):** Simulation of flow for SET 01, 02, 03, 04 (Variation in LBE flow rate with nitrogen flow rate and carry under in down comer zone.
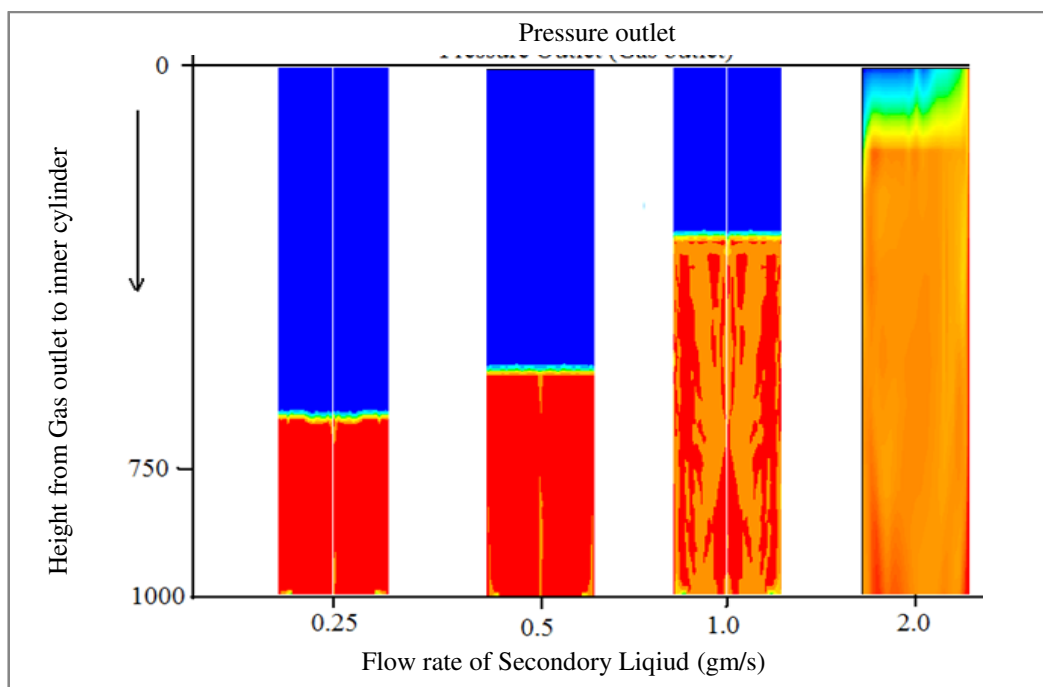


**Figure-2**(b)**:** Simulation of flow for SET 01, 02, 03, 04 (Height of free surface of liquid increases as the flow rate increases).
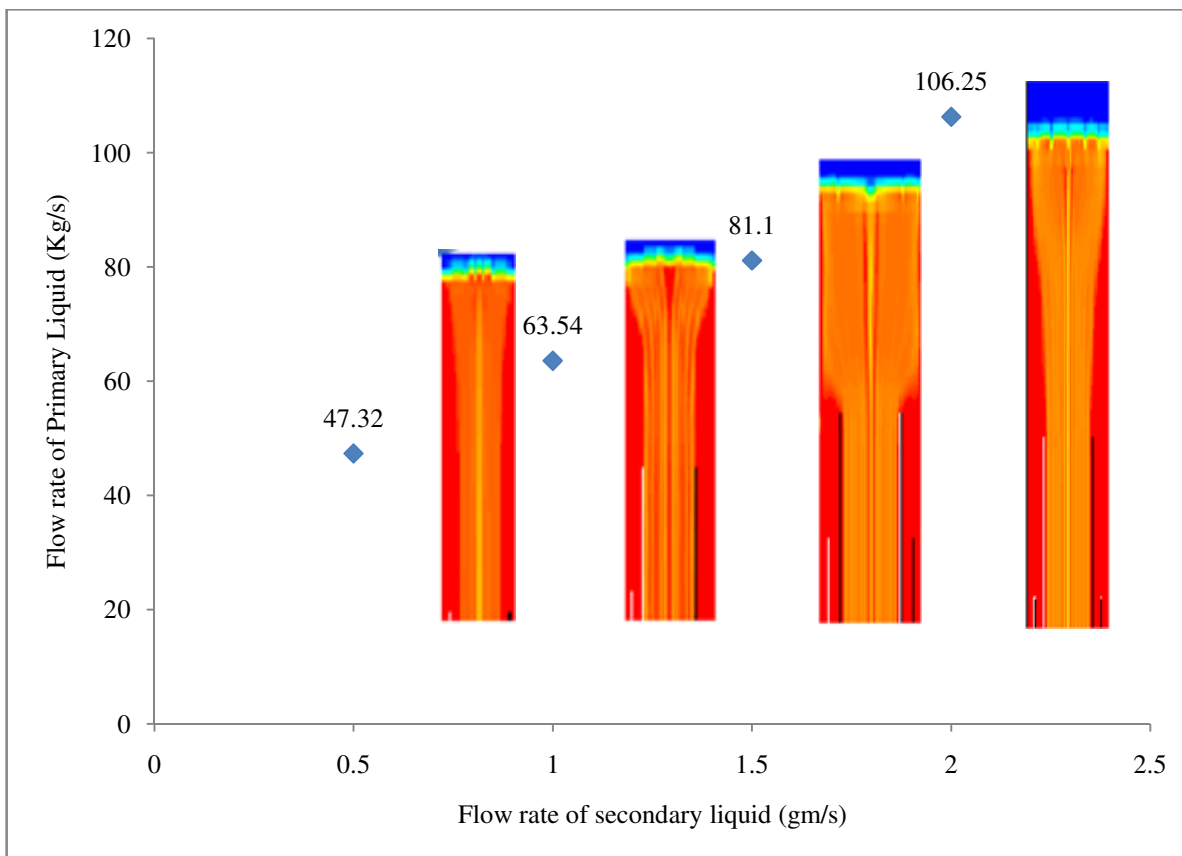
**Figure-3:** Simulation of flow for SET 05, 06, 07, 08, 09 (Variation in LBE flow rate with nitrogen flow rate).



**Figure-4(a):** Simulation of flow for SET 10, 11, 12, 13, 14, 15 (Variation in LBE flow rate with nitrogen flow rate). (b)Variation in LBE flow rate by varying bubble diameter).
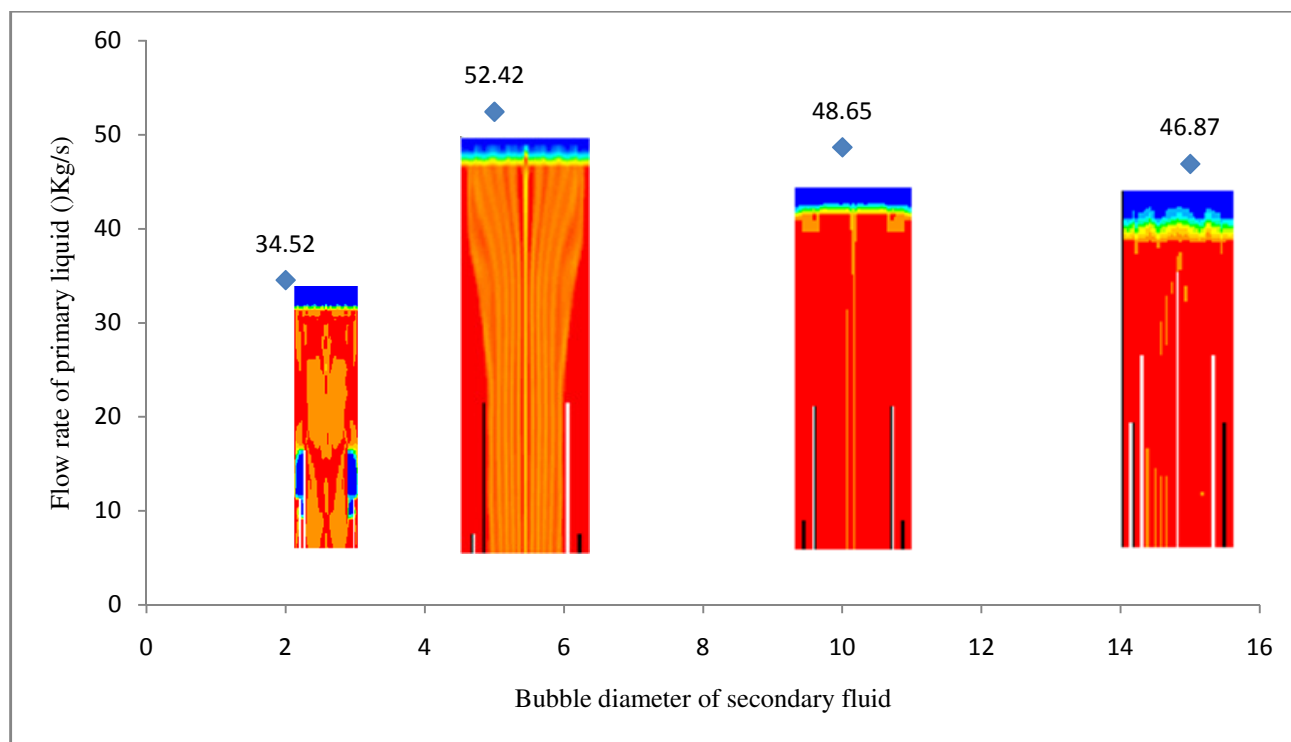
**Figure-4(b)**: Variation in LBE flow rate by varying bubble diameter).

From Figure-3 it can be seen the flow behavior of LBE when the gap of down comer zone was increased from 22 to 44 mm, because for small opening of gas outlet pressure drop was more due to this back pressure was developed at down comer zone that was not allowing the gas to go out, means some gas was trapped at down comer zone but in second case when outlet opening was changed to 20 mm, pressure was approximately equal the atmospheric pressure, as a result this gas can easily go out. Further when the geometry were changed from the previous set to new set (SET 10 to SET 15), in this case Maximum flow rate of LBE was up to 105 kg/s without carry-under, at flow rate of Nitrogen is 2.2 gm/s carry-under occurs and LBE flow rate decreased as shown in Figure-5 because due to carry-under, there was additional pressure drop. Carry-under can be removed if again the flow rate is reduced from 2.2 to 2 gm/s.

**Optimized geometry for ADS target loop:** In ADS system, other things have to be installed such as water jacket etc. For that purpose new geometry was considered where the gap between inner and outer cylinder was reduced from 44 mm to 33 mm means total radius of target loop is 98 mm. All dimensions are same as third case and simulation was done keeping all the setting of fluent same as previous case. At 15.0 mm bubble diameter of nitrogen flow rate of LBE is 46 Kg/s. This flow rate increases by decreasing the bubble diameter and get maximum flow rate 51.5 kg/s was obtained at 5 mm bubble diameter.

For SET 08, 09, 14, 15 slip were not calculated because of high amount of carry over in the down-comer zone so for the mentioned SET of data were not taking part in the optimization of geometry.

## Conclusion

It can be concluded that for continuous flow gas lift optimization process CFD studies could be a better option as it can be used to determine the correct gas injection and the optimum flow rate in gas lift system, Gas lift system is able to increase circulation of liquid. In this project work detailed analysis of gas driven ADS target has been carryout for different geometry, for different flow rate of gas and for different bubble diameter etc to arrive at optimum target configuration. The flow model includes free surface determination, carry-under and carry-over phenomena.

This analysis indicates beyond certain flow rate for a given geometry, carry-under of gas takes place in the down-comer. The carry-under gas, blocks part of down-comer flow area, leading to additional pressure drop and consequently decrease in the liquid metal flow rate. Thus we found an optimum liquid metal flow rate for a given geometry.

The analysis also indicates sensitivity of carry-under on exit gas flow area in the separator. For a 5mm gas out let, at higher flow rates, the separator pressure was more due to large pressure drop in the gas exit. Due to this, there was significant increase in the carry-under, leading to drop in the liquid metal flow rate. Based on the work carried out here, optimum target geometry, gas flow rate have been estimated for the proposed.

**Table-4:** Slip variation with different SET of Configuration.

| For SET 01, 02, 03, 04 | | | | |
|---|---|---|---|---|
| Distance from mixture (mm) | Nitrogen 0.5 gm/s | Nitrogen 1.0 gm/s | | Nitrogen 1.5 gm/s |
| 340 | 1.603426073 | 1.932323724 | | 1.62774599 |
| 1820 | 1.632217093 | 2.275615059 | | 2.727291327 |
| 2940 | 1.629117942 | 2.47085484 | | 2.629819529 |
| 3980 | 2.133713601 | 2.496867679 | | 2.628671201 |
| **For SET 04, 05 ( constant N$_2$ flow rate - 0.5 gm/s)** | | | | |
| | | Gas outlet opening (mm) | | |
| | | 5 mm | 20 mm | |
| 340 | | 1.065097877 | 1.294593091 | |
| 1820 | | 1.14429329 | 1.351337473 | |
| 2940 | | 1.238028674 | 1.378924759 | |
| 3980 | | 1.481709454 | 1.461059421 | |
| **For SET 06, 07 (constant Gas outlet opening 20 mm )** | | | | |
| 340 | | 1.065097877 | | 1.269143222 |
| 1820 | | 1.144293288 | | 1.416162461 |
| 2940 | | 1.238028674 | | 1.501407431 |
| 3980 | | 1.481719403 | | 1.568953087 |

| For SET 10, 11, 12, 13 | | | | |
|---|---|---|---|---|
| Distance from mixture (mm) | Nitrogen 0.5 gm/s | Nitrogen 1.0 gm/s | Nitrogen 1.5 gm/s | Nitrogen 2.0 gm/s |
| 340 | 1.740618185 | 1.621364016 | 1.565355306 | 1.522615 |
| 1820 | 1.851825789 | 1.694241767 | 1.651644028 | 1.602383 |
| 2940 | 1.90402666 | 1.724052323 | 1.679970465 | 1.632068 |
| 3980 | 1.951434699 | 1.709065272 | 1.678148649 | 1.63218 |
| **For SET 16, 17, 18, 19** | | | | |
| 340 | 1.907341033 | 1.772411163 | 1.610608338 | 1.644599 |
| 1820 | 1.9809347 | 1.845645115 | 1.747453532 | 1.721484 |
| 2940 | 2.000681492 | 1.864727015 | 1.748879682 | 1.700775 |
| 3980 | 2.000640497 | 1.86546547 | 1.789503969 | 1.775892 |

| For SET 17, 20, 21, 22 (constant N$_2$ flow rate – 1.0 gm/s) | | | | | | |
|---|---|---|---|---|---|---|
| | | Gas Bubble Diameter (mm) | | | | |
| | | 2.5 | 5.0 | 10 | 15 | |
| 340 | | 1.506 | 1.611 | 2.137 | 2.168 | |
| 1820 | | 1.694 | 1.747 | 2.215 | 2.429 | |
| 2940 | | 1.693 | 1.749 | 2.231 | 2.505 | |
| 3980 | | 1.814 | 1.790 | 2.252 | 2.596 | |

# References

1. Rubbia C., Rubio J.A. and Buono S. (1997). CERN-group conceptual design of a fast neutron operated high power energy amplifier (IAEA-TECDOC--985). *International Atomic Energy Agency (IAEA)*, Vienna, 29(13), 187-312.

2. Satyamurthy P., Gantayet L.M. and Ray A.K. (2007). Heavy density liquid metal spallation target studies for indian ADS programme. *Pramana - J Phys*, 68(2), 343-353. https://doi.org/10.1007/s12043-007-0039-z.

3. Arul Prakash K., Biswas G. and Rathish Kumar B.V. (2006). Numerical simulation of the target system of an ADSS. *International journal of Computational Fluid Dynamics*, 20(7), 513-520. http://dx.doi.org/10.1080/10618560600971754

4. Naik H., Prajapati P.M., Surayanarayana S.V., Jagadeesan K.C., Thakare S.V., Raj D. and Mukherjee S. (2011). Measurement of the neutron capture cross-section of 232 Th using the neutron activation technique. *The European Physical Journal A-Hadrons and Nuclei*, 47(4), 1-9. https://doi.org/10.1140/epja/i2011-11051-2

5. Mantha V., Mohanty A.K. and Satyamurthy P. (2007). Thermal hydraulic studies of spallation target for one-way coupled indian accelerator driven systems with low energy proton beam. *Pramana - J Phys*, 68(2), 355-363. https://doi.org/10.1007/s12043-007-0040-6

6. Tawar R., Sameer S., Pal S., Nambiar P. and Satyamurthy P. (2006). Simulation Studies Related to Window Heating of Spallation Target for ADS. 33rd National and 3rd International Conference on Fluid Mechanics and Fluid Power. IIT Bombay, India.

7. Yasin S.S.M., Aziz N.M.A.N., Zakaria Z. and Samsuri A. (2014). A Study of Continuous Flow Gas Lift System Using CFD. *Journal of Applied Sciences*, 14, 1265-1270. https://doi.org/10.3923/jas.2014.1265.1270

8. Mishra Santosh, Chandra H. and Arora A. (2012). Solid Liquid Non-Newtonian fluid flow in pipe: a Review. *Acta Mechanica Slovaca*, 16(2), 62-73.

9. Cazarez-Candia O. and Mendoza-Maya P. (2009). Modeling of Two-Phase Flow in Oil Wells Using a Simplified Two- Fluid Model. *Petroleum Science and Technology*, 27(17), 1959-1971. http://dx.doi.org/10.1080/10916460802624047

10. FLUENT ANSYS (2009). User's Guide. http://users.ugent.be/~mvbelleg/flug-12-0.pdf. 03/02/2017.

11. Kulkarni A.A., Ekambara K. and Joshi J.B. (2007). On the development of flow pattern in a bubble column reactor: Experiments and CFD. *Chemical engineering science*, 62(4), 1049-1172. https://doi.org/10.1016/j.ces.2006.10.011

12. Bowen R.M. (1976). Theory of mixtures in Continuum Physics. A.C. Eringen, Ed., 3, 1-317, Academic Press, New York, NY, USA.

13. Smith B.L., Dury T.V., Ni L. and Zucchini A. (2008). Computational Fluid Dynamic Studies of the MEGAPIE Spallation Source Target and Safety Vessel. *Journal of nuclear science and technology*, 45(12), 1334-1346. https://doi.org/10.1080/18811248.2008.9711921.